Theory of THz emission from optically excited semiconductors in crossed electric and magnetic fields

G. Meinert, L. Bányai, P. Gartner,* and H. Haug
Institut für Theoretische Physik, J. W. Goethe-Universität Frankfurt, Robert-Mayer-Strasse 8, D-60054 Frankfurt a.M., Germany
(Received 1 February 2000)

The coherent transients generated by femtosecond interband photoexcitation of a semiconductor in crossed electric and magnetic fields are calculated. The scattering with LO phonons is considered and the complex interplay between excitation and dephasing is analyzed. While below the LO-phonon threshold the signal is not effectively damped, above the threshold damping takes place on a picosecond time scale, in qualitative agreement with corresponding experiments.

I. INTRODUCTION

Within the last decade considerable efforts have been devoted to the search for terahertz (THz) emitters as well as to the use of this radiation as a method of condensed matter spectroscopy. In this context a new research topic known as the dynamical Franz-Keldysh effect[1–5] developed. Several mechanisms have been proven to generate THz signals: coherent phonons,[6,7] optical rectification and instantaneous polarization[8–12] in magnetic fields,[13–15] cold plasma oscillations,[16] asymmetric double quantum wells,[17–19] heavy–light-hole beatings in quantum wells,[17,20] and Bloch oscillations in superlattices.[21–23] As different as these mechanisms are in detail, they all are footed on common ground: In a system with broken symmetry it is possible to create coherent wave packets by short laser pulses. When the wave packets are charged, the motion of the wave packets gives rise to a time-dependent dipole moment and a corresponding emission of electromagnetic radiation in the form of THz oscillations. With respect to emitter applications, the tunability and the amplitudes of the signals, as well as the damping of the oscillations, are of crucial interest.

In the present paper we show how THz radiation can be generated in bulk material exposed to perpendicular electric and magnetic fields, known as the Voigt geometry. Here the electric field serves to break the symmetry so that the optical excitation leads to a coherent generation of electrons and holes, while the frequency of the oscillations is determined by the magnetic field, which can be tuned readily. As the dominant damping process we investigate the interaction with LO phonons by calculating quantum-number-dependent transverse relaxation times. A main feature of our analysis is that these relaxation times are not taken as phenomenological fit parameters but are calculated microscopically. It has been found[27–29] that the relaxation time is considerably larger than that without applied fields. Our calculated relaxation times yield an explanation for the observed THz signals on a picosecond time scale. Furthermore, the complex interplay of excitation and the various transverse relaxation times could not be described by a simple classical model with a constant damping term.

The paper is organized as follows: First we diagonalize the one-particle Hamiltonian in the crossed fields and formulate the optical excitation and the scattering due to LO phonons in this representation. Then we derive the kinetic equations on a reduced subset of quantities, sufficient to express the current connected with the THz radiation. Finally we present numerical results and discuss them with respect to experimental observations.

II. THE REPRESENTATION OF A SHIFTED OSCILLATOR

For a magnetic field in the z direction and an electric field in the x direction, the Hamiltonian for an electron or hole $(i=e,h)$ is in the asymmetric Landau gauge $\vec{A}=x\mathcal{B}\vec{e}_y$, where $\vec{e}_y$ is a unit vector in the y direction, given by

$$H^i=\frac{1}{2m_i}\left(\frac{\hbar}{i}\vec{\nabla}-e^i\vec{e}_y x\mathcal{B}\right)^2-e^i\mathcal{E}x. \tag{2.1}$$

Because the potential energy depends only on the x coordinate, one can use plane waves in the y and z directions:

$$\psi(\vec{r})=\frac{e^{i(k_z z+k_y y)}}{\sqrt{L_z L_y}}\phi(x). \tag{2.2}$$

The resulting Hamiltonian for $\phi(x)$ is bilinear in x and can be put into the form

$$H^i=\frac{\hbar^2 k_z^2}{2m_i}-\frac{\hbar^2 d^2}{2m_i dx^2}+\frac{1}{2}m_i\omega_c^{i2}(x-X^i)^2-e^i\mathcal{E}X^i+\frac{(e\mathcal{E})^2}{2m_i\omega_c^{i2}}, \tag{2.3}$$

where the spatial shift of the oscillator origin is

$$X^i=\frac{e^i}{e}l^2k_y+\frac{e^i\mathcal{E}l^2}{\hbar\omega_c^i}. \tag{2.4}$$

The cyclotron frequency ω_c^i and the magnetic length l are given by

$$\omega_c^i=\frac{e\mathcal{B}}{m_i},\quad l^2=\frac{\hbar}{e\mathcal{B}}. \tag{2.5}$$

In these formulas the electron and hole charges are $e^e=-e$ and $e^h=e$, respectively. The eigenfunctions are given by shifted oscillator eigenfunctions

$$\psi^i(\vec{r})=\frac{e^{i(k_z z+k_y y)}}{\sqrt{L_z L_y}}\phi_n(x-X^i), \tag{2.6}$$

where

$$\phi_n(x)=\frac{1}{\sqrt{\sqrt{\pi}l2^n n!}}e^{-x^2/2l^2}H_n(x/l),$$

$$H_n(x)=(-1)^n e^{x^2}\frac{d^n}{dx^n}e^{-x^2}, \tag{2.7}$$

and the spectrum is

$$\epsilon^i_{n,X,k_z}=\frac{\hbar^2 k_z^2}{2m_i}+\hbar\omega_c^i(n+\tfrac{1}{2})-e^i X^i\mathcal{E}+\frac{e^2\mathcal{E}^2}{2m_i\omega_c^{i2}}, \tag{2.8}$$

which is composed of the kinetic free-particle energy in the z direction, the Landau energies, and two corrections due to the electric field. Note that the effect of the electric field is twofold: First the degeneracy of the energies with respect to X is lifted and second the shift in the wave functions becomes mass dependent.

Using this shifted oscillator basis we now treat the coupling to the light field. Because the optical wavelength is typically larger than l, the interband polarization has to be averaged spatially. Within the slowly varying envelope approximation, the averaged polarization is

$$P(t)=\frac{d}{V}\int d^3r\langle\hat{\Psi}_h(\vec{r},t)\hat{\Psi}_e(\vec{r},t)\rangle+\text{H.c.}, \tag{2.9}$$

where d is the matrix element between the Bloch states of the conduction and the valence band close to the band edge. For the optical transitions the momentum components are conserved, i.e., $k_z=-k_z'$, $k_y=-k_y'$, where the $\vec{k}$, $\vec{k}'$ wave vectors refer to the electron and hole, respectively. a^i_{n,X,k_z} are the annihilation operators for a particle i in the state n,X,k_z. Because the excitation is diagonal in k_y, the shift quantum numbers X differ for electrons and holes due to the field term,

$$X_e=-l^2k_y-\frac{|e|\mathcal{E}l^2}{\hbar\omega_c^e},\quad X_h=-l^2k_y+\frac{|e|\mathcal{E}l^2}{\hbar\omega_c^h}. \tag{2.10}$$

Thus the field operators for the electron and the hole $\hat{\Psi}_i(\vec{r},t)$ in the overlap integral are shifted differently. Expanding the field operators into the eigenfunctions (2.6) one gets

$$P(t)=\frac{d}{V}\sum_{n,n',X,k_z}C(\xi)_{nn'}\langle a^h_{n',X+\xi,-k_z}(t)a^e_{nXk_z}(t)\rangle+\text{H.c.}, \tag{2.11}$$

with $C(\xi)_{nn'}=\int dx\,\phi_n(x)\phi_{n'}(x-\xi)$, where $\xi=|e|\mathcal{E}l^2/\hbar\omega_c$ with $1/\omega_c=1/\omega_c^e+1/\omega_c^h=(m_e+m_h)/|e|B$. Again the effect of the electric field is twofold: Equation (2.11) shows that the creation and annihilation of the electron-hole pair is nonlocal (a hole is created at $X+\xi$ while the electron is created at X). This effect has been well examined in the purely electric case ($\mathcal{B}=0$), where it is known as optical rectification.[8] Moreover, the selection rules known from the purely magnetic case[24] ($\mathcal{E}=0$) are destroyed: the optical matrix element may be nondiagonal in the Landau-level quantum numbers. From the overlap integral one sees that the orthogonality of the shifted oscillator functions no longer applies, because the shift of the wave functions is different for electrons and holes. This point is crucial for our analysis: Only due to the symmetry-breaking effect of the electrical field does it become possible to excite wave packets with short pulses, which would otherwise be forbidden by the selection rules. As will be discussed later these wave packets and the corresponding intersubband polarization give rise to THz signals.

At low densities, where the electron-electron interaction can be neglected, the interaction with LO phonons is the dominant scattering mechanism. This interaction is usually modeled in the basis of plane waves by the Fröhlich coupling. To adapt this coupling to the Voigt geometry the shifted oscillator functions are expanded in terms of plane waves in order to calculate the matrix elements. Fermi's golden rule yields the transition rates

$$W^{\vec{q},i}_{n,X,k_z;n',X',k_z'}=\frac{2\pi C^i}{\hbar L_x L_y L_z}[1+N(\hbar\omega_{LO})]\,\delta(\epsilon^i_{nXk_z}-\epsilon^i_{n'X'k_z'}-\hbar\omega_{LO})$$
$$\times\delta_{q_y,k_y-k_y'}\delta_{q_z,k_z-k_z'}\frac{\left|\int dx e^{iq_x x}\phi_n(x)\phi_{n'}(x-(X-X'))\right|^2}{q_x^2+(1/l^4)(X-X')^2+(k_z-k_z')^2}, \tag{2.12}$$

with

$$C^i=\alpha_i\frac{4\pi\hbar(\hbar\omega_{LO})^{3/2}}{(2m_i)^{1/2}},$$

where

$$\alpha_i=\frac{e^2}{\hbar}\left(\frac{m_i}{2\hbar\omega_0}\right)^{1/2}\left(\frac{1}{\epsilon_\infty}-\frac{1}{\epsilon_0}\right)$$

is the dimensionless Fröhlich polaron coupling constant and m_i the effective mass of the electrons and holes; $N(\hbar\omega_{LO})=1/(e^{\beta\hbar\omega_{LO}}-1)$ is the thermal phonon distribution. The transition rates for the phonon absorption can be obtained

through the ''detailed balance'' relation from the given rate due to the phonon emission process.

These transition rates can now be used to write the full collision terms for a Boltzmann scattering. Instead of treating the full kinetics of the density matrix elements, we will take only the dephasing of the off-diagonal elements by relaxation times into account. For this purpose we calculate the probability (per time) to scatter from a given state into all other states (neglecting the fact that this state may be occupied already). Summing over all possible scattering channels the result is a quantum-number-dependent inverse transverse relaxation time

$$\frac{1}{\tau^i_{nXk_z}}=\frac{1}{\tau^i_{nk_z}}=\sum_{n'X'k'_z}\sum_{\vec{q}} W^{\vec{q},i}_{n,X,k_z;n',X',k'_z}. \tag{2.13}$$

Thus all scattering processes give rise to exponential decays. The corresponding characteristic times are individually calculated for any set of quantum numbers.

III. DERIVATION OF THE KINETICS ON A REDUCED SUBSET

Postponing the scattering kinetics for a moment and putting all quantum numbers n,X,k_z in one multi-index ν, the Hamiltonian for the electron-hole system interacting with a coherent light pulse is

$$H=\sum_\nu (\epsilon^e_\nu a^{e\dagger}_\nu a^e_\nu+\epsilon^h_\nu a^{h\dagger}_\nu a^h_\nu) - \frac{1}{2}\left[dE_0(t)e^{i\omega t}\sum_{\nu\nu'} C_{\nu\nu'}a^h_{\nu'}a^e_\nu+\text{H.c.}\right], \tag{3.1}$$

where $E_o(t)$ is the amplitude of the femtosecond pulse and ω is the central frequency. For the electron and hole subband density matrix elements we define $f^i_{\nu\nu'}\equiv\langle a^{i\dagger}_\nu a^i_{\nu'}\rangle$ with $i=e,h$. One has to distinguish between populations ($\nu=\nu'$) and intersubband polarizations ($\nu\neq\nu'$) by the index combination. The interband polarization components are defined as $P_{\nu\nu'}\equiv e^{-i\omega t}\langle a^h_\nu a^e_{\nu'}\rangle$. In the rotating-wave approximation the equations of motion are

$$\left(\frac{\partial}{\partial t}-\frac{i}{\hbar}(\epsilon^e_\nu-\epsilon^e_{\nu'})\right)f^e_{\nu\nu'}=-\frac{i}{2}\sum_{\mu\mu'} C_{\mu\mu'}(\Omega_R\delta_{\mu\nu}P_{\mu'\nu'} - \Omega_R\delta_{\mu\nu'}P^*_{\mu'\nu}), \tag{3.2}$$

$$\left(\frac{\partial}{\partial t}-\frac{i}{\hbar}(\epsilon^h_{\nu'}-\epsilon^h_\nu)\right)f^h_{\nu\nu'}=-\frac{i}{2}\sum_{\mu\mu'} C_{\mu\mu'}(\Omega_R\delta_{\mu'\nu}P_{\nu'\mu} - \Omega_R\delta_{\nu'\mu'}P^*_{\nu\mu}), \tag{3.3}$$

$$\left(\frac{\partial}{\partial t}+\frac{i}{\hbar}(\epsilon^e_{\nu'}+\epsilon^h_\nu-\omega)\right)P_{\nu\nu'}=\frac{i}{2}\Omega_R\sum_{\mu\mu'} C_{\mu\mu'}(\delta_{\nu'\mu}\delta_{\nu\mu'} - \delta_{\mu'\nu}f^e_{\mu\nu'}-\delta_{\nu'\mu}f^h_{\mu'\nu}), \tag{3.4}$$

where $\hbar\Omega_R(t)=dE_0(t)$ is the Rabi frequency. In these equations two consequences of the symmetry-breaking effect of the electric field are easily observed. While the equations for the intraband matrix elements of electrons and holes are normally equal, they differ here by the coupling to the interband polarization via the optical field. Even more important is the observation that the intersubband polarization components $f^i_{\nu\nu'}$ are excited at all.[25,26] In the next paragraph it will be shown that this intersubband polarization is closely related to the THz signal. Thus it is the electric field in the Voigt geometry that allows the THz emission. In order to handle the large number of density matrix elements caused by the appearance of the intersubband polarizations $f^i_{\nu\nu'}$, an approximation scheme will be introduced, which is based on the properties of the optical matrix element. We showed that $C_{\nu,\nu'}=C_{n,n'}\,\delta_{X',X-\xi}\,\delta_{k_z,-k'_z}$. Although there is no longer a selection rule in the Landau levels, still the conservation of momentum enforces $\delta_{k_z,-k'_z}$ and the shift in the quantum number X to be fixed through $\delta_{X',X-\xi}$. Applying these rules to the equations one ends with a closed subset of equations. It has to be emphasized that this subset is closed as long as only the coherent part (3.2) to (3.4) is considered and scattering processes are neglected. On the other hand, the collision terms couple to quantities not initially induced by the light field. In this approximation these quantities are considered to be of minor importance. Into this reduced set, we insert finally in the quantum-number-dependent transverse relaxation times.

With the definitions $f^i_{nXkn'Xk}=f^i_{nn'Xk}$, $P_{nXkn',X-\xi,-k}=P_{nn',X-\xi/2,k}$, the equations become

$$\left(\frac{\partial}{\partial t}-i\nu^e\right)f^e_{nn',X-\xi/2,k}=-\frac{i}{2}\sum_m (C_{nm}\Omega_R P_{mn',X,-k} - C_{n'm}\Omega_R P^*_{mn,X,-k}) + \left.\frac{\partial}{\partial t}\right|_{coll} f^e_{nn'Xk}, \tag{3.5}$$

$$\left(\frac{\partial}{\partial t}-i\nu^h\right)f^h_{nn',X+\xi/2,k}=-\frac{i}{2}\sum_m (C_{mn}\Omega_R P_{n'm,X,k} - C_{mn'}\Omega_R P^*_{nm,X,k})+\left.\frac{\partial}{\partial t}\right|_{coll} f^h_{nn'Xk}, \tag{3.6}$$

$$\left(\frac{\partial}{\partial t}+i\nu^P\right)P_{nn'Xk}=\frac{i}{2}\Omega_R\left(C_{n'n}-\sum_m (C_{mn}f^e_{mn',X-\xi/2,-k} + C_{n'm}f^h_{mn,X+\xi/2,k})\right)+\left.\frac{\partial}{\partial t}\right|_{coll} P_{nn'Xk}, \tag{3.7}$$

$$\left.\frac{\partial}{\partial t}\right|_{coll} f^i_{nn'X\mp(\xi/2)k}=-\frac{f^i_{nn'X\mp(\xi/2)k}}{\frac{1}{2}(\tau^i_{nk_z}+\tau^i_{n'k_z})}\quad(n\neq n'), \tag{3.8}$$

$$\left.\frac{\partial}{\partial t}\right|_{coll} P_{nn'Xk}=-\frac{P_{nn'Xk}}{\frac{1}{2}(\tau^h_{nk_z}+\tau^e_{n'k_z})}. \tag{3.9}$$

Here ν^e, ν^h, and ν^P are defined as

$$\nu^i = \hbar\omega_c^i(n-n'), \quad i=e,h \tag{3.10}$$

$$\nu^P = e^e_{\nu'} + e^h_{h\nu} - \omega = \frac{\hbar^2 k_z^2}{2m_e} + \frac{\hbar^2 k_z^2}{2m_h} + \hbar\omega_c^e(n'+\tfrac{1}{2}) + \hbar\omega_c^h(n+\tfrac{1}{2}) - \frac{E^2}{B^2}\frac{m_c^e+m_c^h}{2} - \Delta, \tag{3.11}$$

where $\Delta=\omega-E_g$ is the detuning, i.e., the energy surplus of the light field with respect to the unrenormalized band gap. Note that there is no thermalization term in the equations with the populations $n=n'$. Due to the electric field the spectrum is not bounded from below if the spectrum is not limited by imposing boundary conditions. Therefore the particles do not relax toward a Fermi function. Populations that do not relax might seem to be a highly unphysical feature on the picosecond time scale we are interested in, but this matches our approximation scheme: The THz signal is generated by the intersubband polarization. With only transverse relaxation times the equations of populations and intersubband polarizations are only coupled on the short time scale of the pulse (on which thermalization is not very effective). After the pulse they decouple and the damping of the intersubband polarization is (in the model) perfectly described by the inverse lifetimes applied to these quantities. The longitudinal relaxation time is of the same order (up to a factor of 2) as the transverse relaxation time. Our calculations show that the transverse relaxation times are in the picosecond range, while the excitation pulses are taken to be 141 fs (full widths at half maximum of the intensity). Because the longitudinal relaxation time is much larger than the duration of the pulse, the approximation is well justified. Izumida *et al.*[13] did experiments with chirped pulses varying the pulse duration. While they observe differences for longer pulses between positive and negative chirp, which suggests occupation effects, there are no discrepancies for pulses of the short duration that we used. This is a confirmation that our approximation without thermalization is well applicable.

IV. THz CURRENT OSCILLATIONS

Charge oscillations and thus current oscillations lead to the emission of electromagnetic dipole radiation. For the inspected THz radiation only intraband contributions are taken into account, i.e., the contributions from the interband polarization are neglected. These contributions are governed by frequencies related to the band gap and are therefore in the optical range.

In the literature on THz radiation without a magnetic field the creation of nonlocal electron-hole pairs has been studied as ''instantaneous polarization'' and a distinction has been made between displacement and transport contribution.[8,10,11,9] All these low-frequency parts are included in the present model, although the displacement current is hardly visible in the range of the considered parameters.

Starting from the definition of the current density operator

$$\vec{J}^i = \frac{1}{V}\int d\vec{r}\,\frac{e^i}{2m_i}\hat{\Psi}_i^\dagger(\vec{r},t)\left[\frac{\hbar}{i}\nabla - e^i\vec{e}_y x\mathcal{B}\right]\hat{\Psi}_i(\vec{r},t) + \text{H.c.} \tag{4.1}$$

one gets by expanding the field operators in the shifted oscillator basis for the current components (again with $i=e,h$):

$$\langle J_z^i\rangle = \frac{e^i}{m_i V}\sum_{n,X,k_z}\hbar k_z f^i_{n,n,X,k_z}, \tag{4.2}$$

$$\langle J_y^i\rangle = -\frac{e^i\mathcal{E}}{\mathcal{B}}\frac{N^i}{V} - \frac{|e|\hbar\sqrt{2}}{m_i l V}\sum_{n,X,k_z}\sqrt{n+1}\,\mathrm{Re}(f^i_{n+1,n,X,k_z}), \tag{4.3}$$

$$\langle J_x^i\rangle = \frac{-e^i\hbar\sqrt{2}}{m_i l V}\sum_{n,X,k_z}\sqrt{n+1}\,\mathrm{Im}(f^i_{n+1,n,X,k_z}). \tag{4.4}$$

Obviously the current in the z direction vanishes, as the effect of the fields is confined to the x-y plane. The first term in the y direction describes a net current proportional to the population. It is mass independent and dependent on the sign of the charges; in the case of charge neutrality (the optical field creates as many electrons as holes) it vanishes. It is of conceptual interest to see that in spite of the electrical field, the coherent motion does not separate electrons and holes on a macroscopic scale. Only the asymmetry in their scattering behavior leads finally to a separation. The influence of this scattering is weak and can be neglected for very low densities. Therefore the electric field does not have to be calculated self-consistently. From Eqs. (4.2) to (4.4) it is obvious that all contributions to the current and to the radiated signal stem from the intersubband polarization. More exactly, the intersubband polarizations for which the Landau-level quantum numbers differ by one are contributing. Reexamining the equations with respect to these quantities, it is immediately clear that they oscillate with nothing but the cyclotron frequency after the femtosecond pulse.

V. NUMERICAL RESULTS AND DISCUSSION

The numerical evaluations are given for GaAs parameters with an LO-phonon energy $\hbar\omega_{LO}=36$ meV. We consider here the contribution of the light holes only, which have been studied also in the corresponding experiments. As all experiments[27–29] were done at low temperatures, in our calculations $T=0$ K is taken for the phonon bath, i.e., only phonon emission is considered. In all results the time integral over the Rabi frequency is taken to be 0.01π, and the full widths at half maximum of the intensity (field squared) is 141 fs (Gaussian pulse shape). Figure 1 shows the inverse lifetime for electrons for the lowest Landau levels as functions of the kinetic energy ($E_{kin}=\hbar^2k_z^2/2m_e$) for a magnetic field $\mathcal{B}=6$ T, where the electron and the light-hole cyclotron energies are $\hbar\omega_c^e=10.5$ meV and $\hbar\omega_c^h=8.5$ meV. In the lowest Landau subband with $n=0$ one sees a smeared-out one-phonon threshold. For the scattering within this subband the threshold becomes flatter with increasing electric field. For the higher Landau subbands the damping increases already at lower kinetic energies because of the transitions to lower subbands. For $n=1$ and $E=6$ kV/cm, one can see

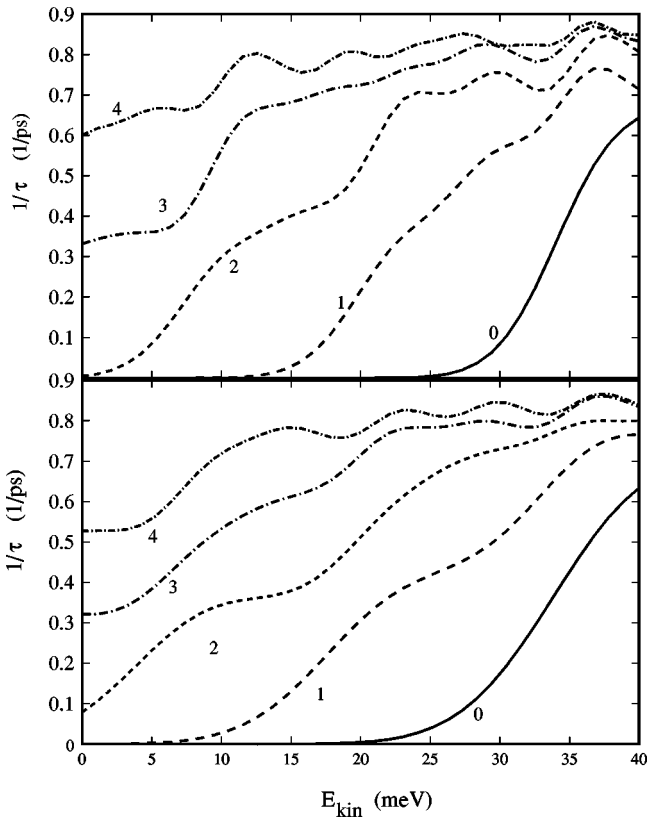

FIG. 1. Inverse of the transverse relaxation times τ^{e}_{n,k_z} for the electrons in various Landau levels versus $E_{kin}=\hbar^2 k_z^2/2m_e$ for a magnetic field $B=6$ T and an electric field $E=4$ kV/cm (upper figure) and $E=6$ kV/cm (lower figure).

clearly first the contributions due to the intersubband scattering by phonon emission to $n=0$, followed by the contributions due to the intrasubband scattering. Because the spectra of the subbands are not bounded from below due to the term $-e^i\mathcal{E}X^i$ intrasubband scattering is at least in principle also possible even at very small kinetic energies $\hbar^2 k_z^2/2m_e$. But due to the localization of the wave function in the magnetic field, scattering over a distance, which is considerably larger than a few magnetic lengths (details are dependent on the shift due to the electric field and the quantum numbers of the wave functions), becomes extremely weak. Because the distance in the scattering process is limited, the energy gained by the nonlocal process in the electric field is restricted also. For the parameters we studied ($4\ \mathrm{T}<\mathcal{B}<8\ \mathrm{T}$, $4\ \mathrm{kV/cm}<\mathcal{E}<6\ \mathrm{kV/cm}$) this energy is by far to small to provide the 36 meV necessary for the emission of a LO phonon. Thus for intrasubband scattering the main contribution has to come from the kinetic energy.

From the calculated relaxation times one expects an approximately undamped motion for excitations below the threshold and damping on a picosecond time scale for above threshold excitations. This result is in agreement with the experimental observations[27–29] of a few resolved cycles of cyclotron radiation on a picosecond time scale.

In Fig. 2 the mean current in the x direction is shown as a function of time and detuning. We limit ourselves to the x component, for its contributions of electrons and holes add up, while in the y direction they work against each other, so that in a model with equal electron and hole masses the y

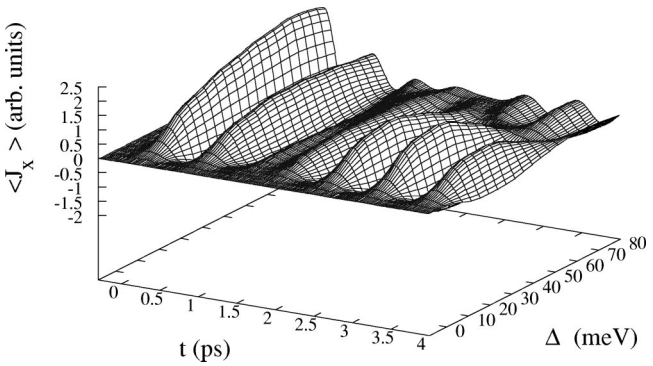

FIG. 2. The time evolution of the x component of the current versus detuning Δ for fixed fields: $E=4$ kV/cm, $B=4$ T.

component of the current would vanish. The two different regimes below and above the threshold are easily recognized. Below threshold there is little damping and so there is a strong beating of electron and hole cyclotron frequencies, but above threshold the situation is more subtle. There is not only a strong damping, but due to the optical excitation of different intersubband polarization components, which differ in sign, partial cancellation occurs. Together with the quantum-number dependence of the transverse relaxation times, the damping of the resulting current is a rather complex interplay of these two effects. One sees, e.g., a revival phenomena: At a certain time total cancellation of all contributions occurs; after the strongly damped parts have died out, only the weakly damped contributions (which are below the one-phonon threshold) survive. By these means the cancellation is lost, and therefore some current reoccurs. The reason for these weakly damped contributions that still exist even for large detunings is the lack of a selection rule in the Landau levels for the optical excitation. For large detuning, a particle (e.g., an electron) can be created high above the threshold, while its counterpart (e.g., a hole) is created in a state below threshold, or vice versa. This explains also why the damping effectively sets in already with a detuning of about one-LO-phonon energy. A similar one-phonon threshold behavior has been seen in the case of Bloch oscillations as well.[30]

All these features are more clearly seen in the Fourier representation of the current (see Fig. 3). The electron and hole cyclotron frequencies appear as separate peaks for low detuning. At about a detuning of an LO-phonon energy,

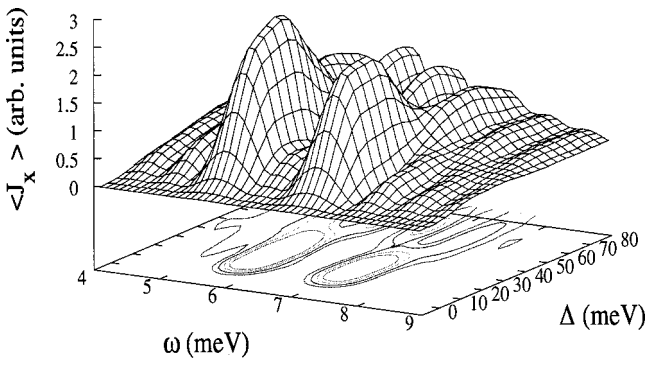

FIG. 3. Spectra of the x component of the current versus detuning Δ for fixed fields: $E=4$ kV/cm, $B=4$ T.

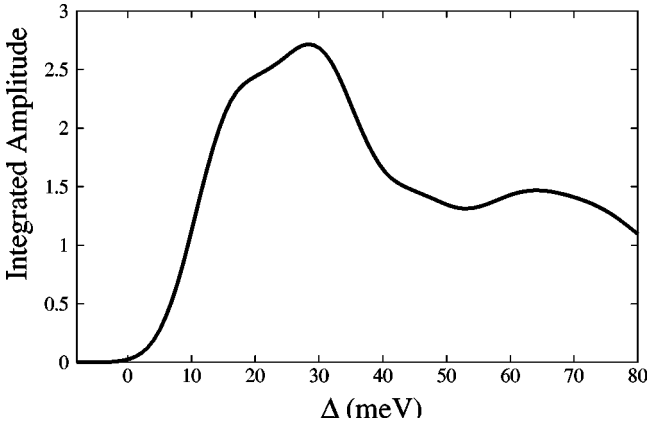

FIG. 4. Integrated square amplitude of the derivative of the current as function of the detuning Δ for fixed fields: $E=4$ kV/cm, $B=4$ T.

damping broadens the peaks, and the competition of different interband polarization contributions causes a crossover from a simple peak structure to a peak-valley-peak structure around both cyclotron frequencies. This can be understood in terms of a superposition of two differently broadened Lorentzians with different signs. Only the additional satellites have no physical meaning, but are numerical artifacts. Although the parameters of our theoretical analysis do not match those of the experiments of Ref. 28, in which only an electric depletion field has been used qualitatively the same features are observed: decay on a picosecond time scale and oscillations with the cyclotron frequencies of electrons and light holes. In Fig. 4 the integrated square amplitude of the time derivative of the current, which is proportional to the radiated signal, is shown. Again this result resembles that of the experiment.[28] A peak for small detunings of about 25–30 meV is followed by a dip. This dip is due to the strong increase of damping for excitations above the LO-phonon energy. In the experimental results, however, the minimum of the dip is reached for twice the LO-phonon energy. This has been explained in terms of the magnetophonon resonance, with the argument that due to the magnetic selection rules both electrons and holes had to be excited above threshold. As shown before, it is a crucial point of our analysis that the selection rules do not hold for $E\neq 0$. Thus for a magnetophonon resonance at $2\hbar\omega_{LO}$ one has to assume the limit of small electric fields, but then the signals would be very weak as well. Because the intrinsic depletion field in the experiment of Ref. 28 has not been under control, further experimental examinations of the field dependence are needed.

VI. CONCLUSION

The mechanism of terahertz generation in a bulk semiconductor in perpendicular electric and magnetic fields has been studied in terms of Bloch equations. We emphasized the importance of the electrical field in breaking the symmetry and inducing the polarization components between various electron or hole Landau subbands. These inter-Landau-subband polarization components are responsible for generating the oscillating current and thus the terahertz signal. Furthermore, the damping of these signals, respectively the current, is analyzed in terms of LO-phonon scattering. As a characteristic quantity, transverse quantum-number-dependent inverse relaxation times have been calculated. A smeared-out one-phonon threshold is obtained, which leads to two different damping regimes: below this threshold regime only a weak damping exists, while above the threshold regime damping on a picosecond time scale is calculated in qualitative agreement with the few available experimental data in this geometry.

ACKNOWLEDGMENTS

The preliminary experimental results of Bauer and Roskos initiated these investigations. We appreciate stimulating discussions with them. This work was supported by the DFG in the framework of the Schwerpunkt *Quantenkohärenz in Halbleitern*.

*Permanent address: National Institute for Physics of Materials, Bucharest, Romania.

[1] Y. Yacoby, Phys. Rev. **169**, 610 (1968).
[2] Y. Rebane, Sov. Phys. Solid State **27**, 824 (1985).
[3] A. P. Jauho and K. Johnsen, Phys. Rev. Lett. **76**, 4576 (1996).
[4] K. B. Nordstrom, K. Johnsen, S. J. Allen, A.-P. Jauho, B. Birnir, J. Kono, T. Noda, H. Akiyama, and H. Sakaki, Phys. Rev. Lett. **81**, 457 (1998).
[5] S. Hughes and D. S. Citrin, Phys. Rev. B **59**, R5288 (1999).
[6] A. V. Kuznetsov and C. J. Stanton, Phys. Rev. B **51**, 7555 (1995).
[7] W. Kütt, G. C. Cho, T. Pfeifer, and H. Kurz, Semicond. Sci. Technol. **7**, B77 (1992).
[8] S. L. Chuang, S. Schmitt-Rink, B. I. Greene, P. N. Saeta, and A. F. J. Levi, Phys. Rev. Lett. **68**, 102 (1991).
[9] A. V. Kuznetsov and C. J. Stanton, Phys. Rev. B **48**, 10 828 (1993).
[10] B. B. Hu, A. S. Weling, D. H. Auston, A. V. Kuznetsov, and C. J. Stanton, Phys. Rev. B **49**, 2234 (1994).
[11] B. B. Hu, E. A. de Souza, W. H. Knox, J. E. Cunningham, M. C. Nuss, A. V. Kuznetsov, and S. L. Chuang, Phys. Rev. Lett. **74**, 1689 (1995).
[12] B. B. Hu, X.-C. Zhang, and D. H. Auston, Phys. Rev. Lett. **67**, 2709 (1991).
[13] S. Izumida, S. Ono, Z. Liu, H. Ohtake, and N. Sarukura, Appl. Phys. Lett. **75**, 451 (1999).
[14] N. Sarukura, H. Ohtake, S. Izumida, and Z. Liu, J. Appl. Phys. **84**, 654 (1998).
[15] H. Ohtake, S. Izumida, Z. Liu, S. Ono, and N. Sarukura, in *Radiative Processes and Dephasing in Semiconductors*, edited by D. S. Citrin, OSA Trends in Optics and Photonics Vol. 18 (Optical Society of America, Washington, D.C., 1998), p. 127.
[16] R. Kersting, K. Unterrainer, G. Strasser, H. F. Kauffmann, and E. Gornik, Phys. Rev. Lett. **79**, 3038 (1997).
[17] M. C. Nuss, P. C. M. Planken, I. Brener, H. G. Roskos, M. S. C. Luo, and S. L. Chuang, Appl. Phys. B: Lasers Opt. **58**, 249 (1994).
[18] K. Leo, J. Shah, E. O. Göbel, T. C. Damen, S. Schmitt-Rink, W. Schäfer, and K. Köhler, Phys. Rev. Lett. **66**, 201 (1991).

[19] H. G. Roskos, M. C. Nuss, J. Shah, K. Leo, D. A. B. Miller, A. M. Fox, S. Schmitt-Rink, and K. Köhler, Phys. Rev. Lett. **68**, 2216 (1992).
[20] P. C. M. Planken, M. C. Nuss, I. Brener, K. W. Goossen, M. S. C. Luo, S. L. Chuang, and L. Pfeiffer, Phys. Rev. Lett. **69**, 3800 (1992).
[21] T. Meier, P. Thomas, and S. W. Koch, Phys. Low-Dimens. Semicond. Struct. **3/4**, 1 (1998), and references therein.
[22] F. Agulló-Rueda and J. Feldmann, in *Semiconductor Superlattices Growth and Electronic Properties*, edited by H. T. Grahn (World Scientific, Singapore, 1995), p. 99.
[23] H. G. Roskos, Adv. Solid State Phys. **34**, 297 (1994).
[24] F. Bassani and G. P. Parravicini, *Electronic States and Optical Transitions in Solids* (Pergamon Press, Oxford, 1975).
[25] M. W. Wu and H. Haug, Solid State Commun. **108**, 809 (1998).
[26] M. W. Wu and H. Haug, Phys. Rev. B **58**, 13 060 (1998).
[27] D. Some and A. V. Nurmikko, Phys. Rev. B **53**, R13 295 (1996).
[28] D. Some and A. V. Nurmikko, Appl. Phys. Lett. **65**, 3377 (1994).
[29] H. G. Roskos (private communication).
[30] G. von Plessen, T. Meier, J. Feldmann, E. O. Göbel, P. Thomas, K. W. Goossen, J. M. Kuo, and R. F. Kopf, Phys. Rev. B **49**, 14 058 (1994).